

# Tracking a Target in Wind Using a Micro Air Vehicle with a Fixed Angle Camera

Jeffery Saunders and Randal Beard

Brigham Young University, Provo, Utah, 84602

**Abstract**—Target tracking in wind with micro air vehicles (MAVs) can be a difficult problem. Traditional tracking systems such as radar are too heavy to mount on a MAV and are often too large for a small airframe. Cameras, laser rangefinders, and ultrasonic sensors provide a viable alternative and are light enough to mount on a MAV. However, each of these sensors are directional and are often mounted at fixed angles requiring airframe control to maintain the sensor on a target. We propose a method of target tracking using a fixed angle camera and derive a closed-loop guidance strategy to fix the target in the image frame using the position and velocity of the target in the image plane to command a heading rate. The resulting motion of the MAV is an elliptical orbit around the target with the target positioned at a focus of the ellipse as predicted in previous open-loop methods.

## I. INTRODUCTION

Fixed wing Micro Air Vehicles (MAVs) are becoming increasingly common in military and civilian use. Their cost continues to decrease even as their functionality increases. During the past ten years, autopilots for MAVs have become possible due to the decreasing size of the necessary sensors as well as the decrease in size and power requirements of integrated circuits. Current autopilots are as small as two inches square and weigh less than an ounce [1]. They may be installed on aircraft with wingspans of less than two feet. These small autonomous aircraft are useful for military and civilian surveillance missions. Small aircraft using onboard cameras can avoid detection because they have a weak audio signal and because the passive camera sensor does not emit detectable energy. In addition, an autopilot facilitates autonomous surveillance. This paper focuses on autonomous surveillance by *target tracking*, defined here as maintaining a target in the field of view of an onboard camera.

Target tracking has a wide range of potential military and civilian uses. Enemy military movements could be automatically tracked by a MAV. The Coast Guard could send a MAV to inspect and track unidentified watercraft. A possible terrorist could be followed with little chance of detection. Police could track suspects without the need for ground vehicles. An automatic target tracking system would be technology enabling in all of these situations.

While target tracking has constructive uses, it can be a difficult problem for a number of reasons. Processing visual data often requires computational resources that are not available on small MAVs, thus requiring a nearby ground station to acquire and process video. Transmitted video is often noisy and intermittent because of transmission interference as well as camera jitter resulting in dropped frames and thus

in noise in the tracked position of the target in the image frame. Therefore the tracking method must be robust to target position error introduced by the camera. Camera motion caused by gusts of wind, or target movement, can cause the target to move outside the camera field of view. This implies the tracking method must also have quick response to target movement in the image plane. Another important question to consider is the feasibility of target tracking. Ignoring fuel constraints, can a target be maintained in the camera field of view indefinitely?

Previous work has addressed some of the problems described in the previous paragraph. For example, Thomasson derived a solution to target tracking in wind [16] by assuming an elevation controlled camera and constant wind. He found that a MAV must fly an ellipse with the target located at one of its foci and the major axis of the ellipse aligned perpendicular to the direction of the wind. The calculation of the dimensions of the ellipse is based on a priori knowledge of the magnitude and direction of the wind velocity. Given the kinematic constraints of the MAV, the wind velocity, and the target velocity, an elliptical trajectory is generated for the MAV to track. As the wind velocity and target velocity remain constant, the MAV may track the target indefinitely. Feedback is not incorporated in the solution, resulting in open-loop target tracking. Problems arise as wind velocity changes, gusts occur, or the target changes course, causing the target to leave the camera's field of view. This paper improves on [16] by incorporating a feedback method where the resulting path in wind is an elliptical orbit around the target.

Successful path planning feedback solutions to target tracking problems have been demonstrated in [10], [6], [15], [11], [3], [4], [14], [13]. The general approach is to generate paths based on current knowledge. As information is acquired, whether about the wind, target, or MAV, the path to track the target is regenerated. Reference [4] generates paths to a landing position based on vision of a runway or other landmark. Moving targets are tracked using dynamic planning in [10], [6], [15], [11], [3], [14] and use gimballed cameras to help track targets. Unfortunately, gimbals are not always feasible on small MAVs. Removing the gimbal introduces additional kinematic constraints and path planning becomes more difficult. Additionally, a gust of wind or a sudden change in course of the target may push the target outside the field of view before a response is generated, possibly causing the MAV to lose the target altogether. Fast response is necessary to prevent the target from leaving the

image plane. A feedback control law using target movement in the image plane may have the response time needed. This paper differs from previous work by utilizing target movement in the image plane to maneuver the MAV such that the target stays in the image plane. Reaction to movement in the image plane generates a fast response preventing the target from leaving the image plane.

A feedback control law is developed in [17] for target tracking from kinematic laws similar to those developed in this paper. The authors assume known target velocity, zero wind, and a gimballed camera. The feedback law tracks a target in simulation and hardware flight tests. The flight paths in [17] were circular trajectories centered around the target. The trajectories were circular rather than elliptical due to the degrees of freedom provided by the gimbal. The gimbal adds weight and may not be feasible on small MAVs. We build on these results by developing a feedback law around the image plane and removing the gimbal.

An adaptive feedback approach to target tracking using computer vision is developed in [7], [8]. A fixed angle camera is used to track a target and an adaptive approach estimates the target velocity and other parameters. This approach had good success in simulation results. Adaptive control however often suffers from transients that affect initial flight performance in hardware tests. A Kalman filter approach integrating a dynamical model and measurements may provide early stability in target state estimation. Feasible Kalman filter approaches to ground target tracking have been shown previously [5].

A common application in target tracking is target geo-location. *Target geo-location* refers to the process of inferring the inertial location of a target from the pose of the sensor and the location of the target in the sensor frame [2], [9]. While target geo-location provides a frame of reference for control, target location error is introduced from error in the estimated pose of the sensor and error in the estimated target location in the sensor frame. If control is based on target movement in the sensor frame rather than the inertial frame, then some error may be bypassed, creating more robust control.

Some of the problems in target tracking methods are addressed in this paper. A non-linear control law is developed using range-to-target and bearing-to-target information obtained from target motion in the image plane. This approach maintains the target in the image plane by providing quick reaction to target movement or gusts of wind. As the target moves in the image plane, the control law "pushes" the target back to the center of the camera field of view. An extended Kalman filter (EKF) reduces noise in estimates. The resulting trajectory in wind as a result of the feedback control law is an elliptical orbit. The goal is to maintain the target in the camera field of view in the presence of wind and target motion.

The organization of this paper is as follows. Section II presents a description of the problem. Section III derives the kinematics of the environment and the control loop. Simulation setup and results are discussed in section IV and

a conclusion is provided in the final section.

## II. PROBLEM DESCRIPTION

The MAV is assumed to have an autopilot with inner control loops to command roll angle, pitch, airspeed, and altitude. The constant altitude kinematic model is therefore given by

$$\dot{z}_n = V_a \cos \psi + V_w \cos \chi_w \quad (1)$$

$$\dot{z}_e = V_a \sin \psi + V_w \sin \chi_w \quad (2)$$

$$\dot{\psi} = \frac{g}{V_a} \tan \phi \quad (3)$$

$$\dot{V}_a = \alpha_V (V_a^c - V_a) \quad (4)$$

$$\dot{\phi} = \alpha_\phi (\phi^c - \phi), \quad (5)$$

where  $(z_n, z_e)^T$  is the position of the aircraft,  $V_g$ ,  $V_a$ ,  $V_a^c$ ,  $\phi$ , and  $\psi$  are the ground speed, air speed, commanded airspeed, roll, and heading,  $\chi$  and  $\chi_w$  are the vehicle course angle and wind angle,  $g$  is the gravitational constant, and  $\alpha_\phi$  and  $\alpha_V$  are positive autopilot parameters. Assuming that the controlled roll dynamics are significantly faster than the heading dynamics (a valid assumption for MAVs), we let

$$\phi^c = \arctan \left( \frac{\dot{\psi} V_a}{g} \right), \quad (6)$$

and think of  $\dot{\psi}$  as the commanded input.

The MAV is equipped with a camera pointed out of the right wing allowing it to persistently orbit a target in the camera field-of-view. The camera is not gimballed and does not move during flight. We assume that vision processing software is available to track the location of the target in the image plane.

Tracking moving targets in wind is difficult because the crab angle caused by wind may move the target out of the camera field-of-view. Currently available sensors on MAVs do not allow accurate measurement of crab angles. GPS sensors allow for measurement of the course angle. The idea pursued in this paper is to use the location of the target in the image plane to track the target. If movement in the image plane could be translated to movement in the aircraft body frame, then the target could be maintained in the center of the image plane. This removes the requirement to measure the crab angle and removes possible error from translations to the world coordinate frame.

## III. CONTROLLING TARGET MOTION IN THE IMAGE PLANE

### A. Relative dynamics and control objective

The relative dynamics are best described by polar coordinates in the MAV body frame. A depiction is shown in figure 1. We assume that a constant relative altitude is maintained by the autopilot. Let  $\rho$  be the range-to-target and

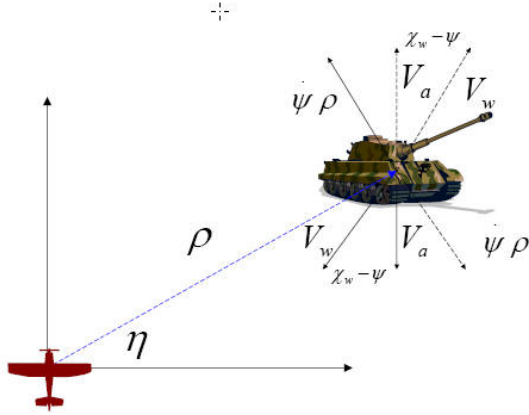


Fig. 1. Dynamics of the target are viewed from the MAV wind frame.

let  $\eta$  be the bearing-to-target. The equations of motion are,

$$\dot{\rho} = -V_a \sin(\eta) - V_w \sin(\eta + \chi_w - \psi) \quad (7)$$

$$\dot{\eta} = \dot{\psi} - \frac{V_a}{\rho} \cos(\eta) - \frac{V_w}{\rho} \cos(\eta + \chi_w - \psi). \quad (8)$$

The control objective is to minimize the distance to the target while simultaneously maintaining the target in the camera field of view, and to do this within reasonable roll angle limits. Formally, the control objectives are

- 1) If  $|\eta(0)| \leq \bar{\eta}$ , ensure that  $|\eta(t)| \leq \bar{\eta}$  for all  $t \geq 0$ , where  $\bar{\eta}$  is the field-of-view of the camera.
- 2) Ensure that  $|\phi(t)| \leq \bar{\phi}$  where  $\bar{\phi}$  is the maximum allowable roll angle.
- 3) Minimize the stand-off distance to the target  $\rho(t)$  to maximize the resolution of the image in the camera frame.

### B. Maintaining the target in the camera field-of-view

To derive a strategy to maintain the target in the camera field of view, consider the Lyapunov function candidate

$$W_1 = \frac{1}{2}\eta^2.$$

Differentiating  $W_1$  along solutions of (8) gives

$$\dot{W}_1 = \eta \left( \dot{\psi} - \frac{V_a}{\rho} \cos \eta - \frac{V_w}{\rho} \cos(\eta + \chi_w - \psi) \right).$$

Selecting the heading rate as

$$\dot{\psi} = \frac{V_a}{\rho} \cos \eta + \frac{V_w}{\rho} \cos(\eta + \chi_w - \psi) - k_1 \eta + \nu, \quad (9)$$

results in

$$\dot{W}_1 = -k_1 \eta^2 + \eta \nu.$$

If  $\theta \in (0, 1)$ , then

$$\begin{aligned} \dot{W}_1 &\leq -k_1 \eta^2 + |\eta| |\nu| \\ &= -(1 - \theta)k_1 \eta^2 + [|\eta| |\nu| - \theta k_1 \eta^2], \end{aligned}$$

which is negative definite if

$$|\eta| \geq \frac{|\nu|}{\theta k_1}.$$

We therefore have the following result.

*Theorem 3.1:* If  $\dot{\psi}$  is given by Equation (9), where

$$|\nu| < k_1 \theta \bar{\eta},$$

where  $0 < \theta < 1$ , then  $|\eta(0)| \leq \bar{\eta}$  implies that  $|\eta(t)| \leq \bar{\eta}$ .

*Proof:* Since  $\dot{W}_1(\bar{\eta})$  and  $\dot{W}_1(-\bar{\eta})$  are both negative, the set  $\{-\bar{\eta} \leq \eta \leq \bar{\eta}\}$  is positively invariant. ■

The signal  $\nu$  will be used later in this section to minimize  $\rho(t)$ .

### C. Roll angle constraint

In this section we will derive an addition bound on  $\nu$  that ensures that the roll angle constraint  $|\phi| \leq \bar{\phi}$  is satisfied.

*Theorem 3.2:* Suppose that  $\rho(t) \geq \underline{\rho}$ ,  $|\eta(t)| \leq \bar{\eta}$ , and that

$$\frac{V_a + V_w}{\underline{\rho}} + k_1 \bar{\eta} < \frac{g}{V_a} \tan \bar{\phi}, \quad (10)$$

and define

$$M(t) = \frac{g}{V_a} \tan \bar{\phi} - k_2 |\eta(t)| - \left( \frac{V_a + V_w}{\rho(t)} \right).$$

If  $|\nu(t)| \leq M(t)$ , then  $|\phi(t)| \leq \bar{\phi}$ .

*Proof:* Condition (10) guarantees that  $M(t) \geq 0$ . From Equation (9) we have

$$\begin{aligned} |\dot{\psi}| &= \left| \frac{V_a}{\rho} \cos \eta + \frac{V_w}{\rho} \cos(\eta + \chi_w - \psi) - k_1 \eta + \nu \right| \\ &\leq \frac{V_a + V_w}{\rho} + k_1 |\eta| + |\nu|. \end{aligned}$$

Since  $\dot{\psi} = \frac{g}{V_a} \tan \phi$ , the roll angle constraint will be satisfied if

$$|\dot{\psi}| \leq \frac{g}{V_a} \tan \bar{\phi}.$$

Therefore, a sufficient condition that ensures that the constraint is satisfied is

$$\frac{V_a + V_w}{\rho} + k_1 |\eta| + |\nu| \leq \frac{g}{V_a} \tan \bar{\phi}. \quad (11)$$

Condition (10) guarantees that there exist values of  $\rho$ ,  $\eta$  and  $\nu$  that can satisfy this inequality. Equation (11) can be rearranged as

$$|\nu| \leq \frac{g}{V_a} \tan \bar{\phi} - \frac{V_a + V_w}{\rho} - k_1 |\eta|. \quad \blacksquare$$

### D. Minimizing the range-to-target

The signal  $\nu$  can be used to minimize the average value of  $\rho$ . In this section we will derive two possible strategies for selecting  $\nu$ . The first strategy is based on a continuous time derivation. Toward that end, let

$$W_2 = \frac{1}{2}(\rho + \lambda \dot{\rho})^2,$$

where  $\lambda > 0$ . Minimizing  $W_2$  will minimize the deviation of  $\rho$  from the origin. Differentiating  $W_2$  gives

$$\dot{W}_2(\nu) = (\rho + \lambda\dot{\rho})(\dot{\rho} + \lambda\ddot{\rho}(\nu)),$$

where

$$\ddot{\rho}(\nu) = (-V_a \cos \eta)\nu + \left[ k_1 V_a \eta \cos \eta + \frac{V_m V_a}{\rho} \cos \eta \cos(\eta + \chi_w - \psi) + \frac{V_w^2}{\rho} \cos(\eta + \chi_w - \psi) \right] \quad (12)$$

is obtained by differentiating Equation (7). Therefore  $\nu$  can be selected as

$$\nu^* = \arg \min_{|\nu| \leq \min\{M(t), k_1 \theta \bar{\eta}\}} \dot{W}_2(\nu) \quad (13)$$

The second strategy for picking  $\nu$  is based on a discrete time version of the dynamics. Substituting Equation (9) into Equation (8) gives

$$\dot{\eta} = -k_1 \eta + \nu. \quad (14)$$

Given a sample rate  $T$ , the sampled-data version of (14) is

$$\eta_{k+1} = e^{-k_1 T} \eta_k + (1 - e^{-k_1 T}) \nu_k.$$

Using an Euler approximation, the sampled-data equivalent of (12) is

$$\rho_{k+2} = \rho_{k+1} + T [-V_a \sin \eta_{k+1} - V_m \sin(\eta_{k+1} + \chi_w - \psi_{k+1})]$$

where

$$\begin{aligned} \rho_{k+1} &= \rho_k + T [-V_a \sin \eta_k - V_m \sin(\eta_k + \chi_w - \psi_k)] \\ \psi_{k+1} &= \psi_k + T \left[ \frac{V_a}{\rho_k} \cos \eta_k + \frac{V_w}{\rho_k} \cos(\eta_k + \chi_w - \psi_k) - k_1 \eta_k + \nu_k \right]. \end{aligned}$$

Therefore,  $\nu_k$  can be selected as

$$\nu_k^* = \arg \min_{|\nu_k| \leq \min\{M_k, k_1 \theta \bar{\eta}\}} \rho_{k+2}.$$

Ref [16] shows that the path of a MAV tracking a target in wind with a roll only camera is an elliptical orbit if  $\eta = 0$ . To show that our approach produces a similar result, divide (7) by (9), letting  $\eta = \nu = 0$  to get

$$\frac{d\rho}{d\psi} = \rho \frac{-V_w \sin(\chi_w - \psi)}{V_a + V_w \cos(\chi_w - \psi)},$$

which, as pointed out in [12] is an elliptical orbit with eccentricity  $\epsilon = \frac{V_w}{V_a}$ . One of the advantages of our approach is that rather than forcing the target to be located along the optical axis, the target is allowed (through the selection of  $\nu$ ) to move in the image plane to facilitate more circular orbits in wind. An interesting question is whether circular orbits, where the target remains in the camera field-of-view, are possible in wind. The following theorem provides explicit conditions.

*Theorem 3.3:* Circular orbits that maintain the target in

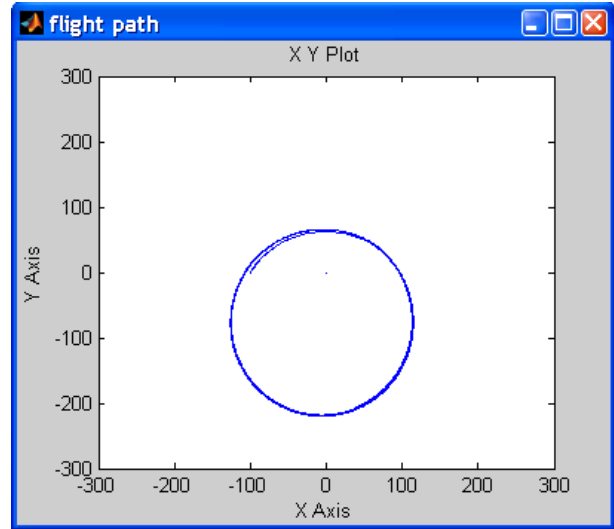


Fig. 2. A flight path of a simulated MAV using the above guidance strategy is shown. The MAV's initial conditions start off the path, but allow the camera to capture the target. The MAV navigates onto a stable path around the target.

the field of view are possible if

$$\tan \bar{\eta} \geq \max_{\psi \in [0, 2\pi]} \left| \frac{\frac{V_w}{V_a} \sin(\chi_w + \psi)}{1 + \frac{V_w}{V_a} \cos(\chi_w + \psi)} \right|.$$

*Proof:* Divide (7) by (9) gives

$$\frac{d\rho}{d\psi} = \rho \frac{-V_a \sin \eta - V_w \sin(\eta + \chi_w - \psi)}{V_a \cos \eta + V_w \cos(\eta + \chi_w - \psi) - k_1 \eta + \nu}.$$

When the orbit is circular,  $\frac{d\rho}{d\psi} = 0$ , or in other words,

$$-V_a \sin \eta - V_w \sin(\eta + \chi_w - \psi) = 0.$$

Solving for  $\tan \eta$  gives

$$\tan \eta = -\frac{\frac{V_w}{V_a} \sin(\chi_w + \psi)}{1 + \frac{V_w}{V_a} \cos(\chi_w + \psi)}.$$

Maximizing the right hand side over all possible values of  $\psi$  gives the desired result. ■

#### IV. SIMULATION RESULTS

Simulations were conducted in Simulink using the equations of motion described in Equations (1)-(5), with  $V_a = 13$  m/s. The location and size of the target in the camera image plane were calculated and sent to the guidance loop, which filtered the inputs and used the strategy described in the previous section.

The results of a stationary target in a constant wind of  $V_w = 7$  m/s to the east are shown in fig. 2. Remember that constant target velocity and constant wind can be generalized to just a constant wind. Notice that the flight path converged to an ellipse as was predicted in [16]. This flight path was the result of a feedback loop that incorporated no previous knowledge of an expected path. The motion of the target in the image plane is shown in figure 3.

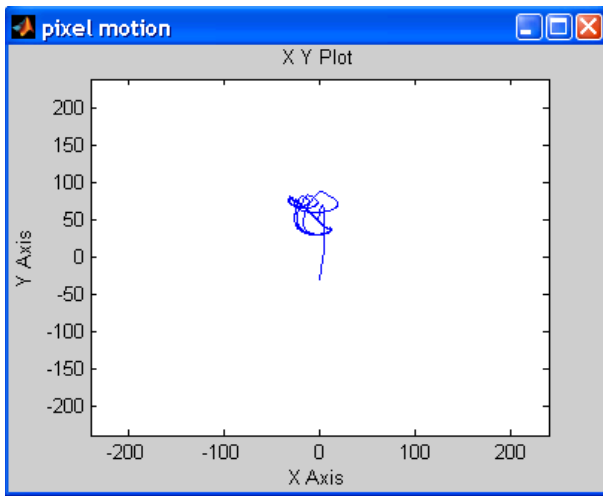


Fig. 3. The motion of the target in the image plane is shown from the flight path in figure 2

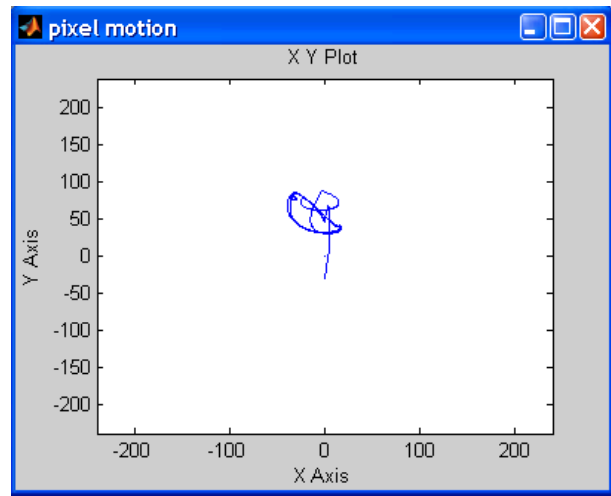


Fig. 5. The motion of the target in the image plane is shown from the flight path in figure 4

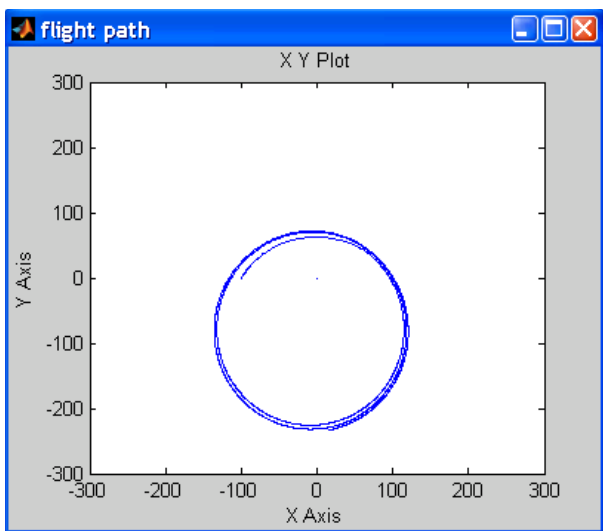


Fig. 4. The simulation result is shown with a high  $k_2$  gain. The resulting path is more circular than a low gain.

To examine the effect of the gain  $k_1$  on the orbital path, the gain was raised allowing the target to move more freely in the image plane and the flight path to be more circular. The result of the simulation is shown in figure 4. The path is more circular as expected. Notice that the target is not centered in the orbit. The control moves the target off the center of the circle as a result of the wind, minimizing the required roll angle to move the target to the center of the image plane, and allowing the MAV to fly a circular path while maintaining the target near the center on the image plane.

To compare to the case without wind, the simulation was run with wind speed equal to zero. The result is displayed in figure 6. The trajectory is circular, and slowly converges to the minimum turn radius as expected. The motion in the

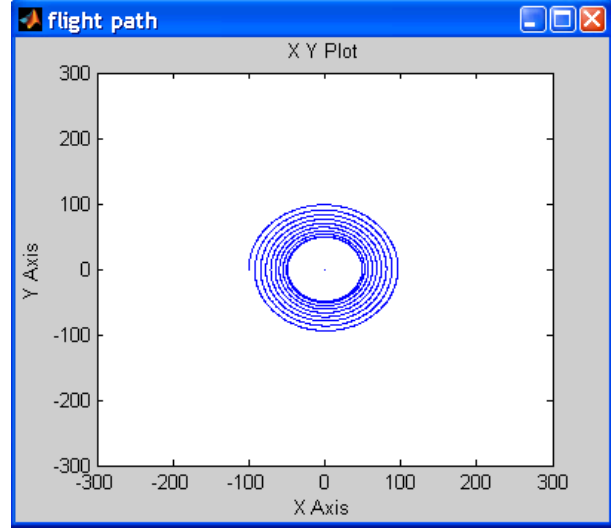


Fig. 6. The simulation result is shown without wind. The resulting path is more circular.

image is small. The target location in the image plane quickly converges to the center of the image plane.

## V. CONCLUSION

In this paper we have derived equations of motion for a target in a MAV body frame of reference and the image plane. In addition we have shown a feasible non-linear feedback method to track a target using image plane target movement in a side-mounted camera. Movement in the image is used to "push" the target in the image plane to maintain it in the camera field-of-view. Simulation results verify the effectiveness of the approach.

## VI. ACKNOWLEDGEMENTS

This research was funded in part by the Air Force Research Laboratory, Munitions Directorate under SBIR con-

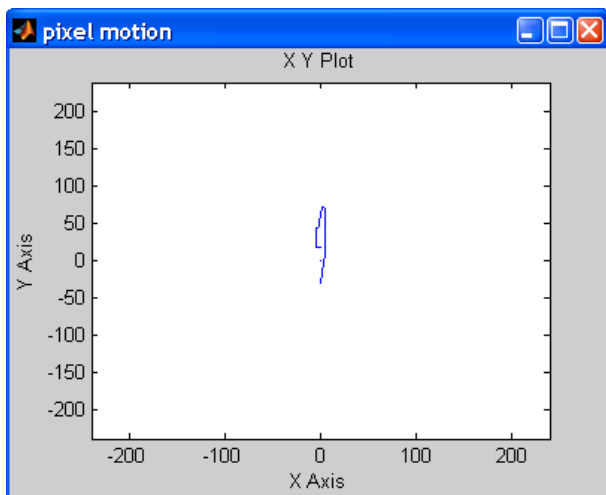


Fig. 7. The motion of the target in the image plane is shown from the flight path in figure 6. There is very little motion.

tract No. FA 8651-07-C-0094 to Scientific Systems Company, Inc. and Brigham Young University. Portions of this work were accomplished while the first author participated in the Air Force Research Laboratory's Summer Research Program at Wright Patterson AFB.

#### REFERENCES

- [1] Randal Beard, Derek Kingston, Morgan Quigley, Deryl Snyder, Reed Christiansen, Walt Johnson, Timothy McLain, and Michael A. Goodrich. Autonomous vehicle technologies for small fixed-wing UAVs. *Journal of Aerospace Computing, Information, And Communication*, 2:92–102, January 2005.
- [2] Allen D.Wu, Eric N. Johnson, and Alison A. Proctor. Vision-aided inertial navigation for flight control. *Journal Of Aerospace Computing, Information, and Communication*, 2(9):348–360, 2005.
- [3] E.W. Frew, X. Xiao, S. Spry, T. McGee, Z. Kim, J. Tisdale, R. Sengupta, and J. K. Hendrick. Flight demonstrations of self-directed collaborative navigation of small unmanned aircraft. In *AIAA 3rd Unmanned Unlimited Technical Conference*, September 2004.
- [4] Ruggero Frezza and Claudio Altafini. Autonomous landing by computer vision: an application of path following in SE(3). In *Conference on Decision and Control*, December 2004.
- [5] Sudesh Kumar Kashyap, Girija G., and J.R. Raol. Evaluation of converted measurement and modified extended Kalman filters for target tracking. In *AIAA Guidance, Navigation and Control Conference and Exhibit*, August 2003.
- [6] Jusuk Lee, Rosemary Huang, Andrew Vaughn, Xiao Xiao, and J. Karl Hedrick. Strategies of path-planning for a UAV to track a ground vehicle. In *Proceedings of the 2nd Annual Autonomous Intelligent Networks and Systems Conference*, 2003.
- [7] L. Ma, C. Cao, V. Dobrokhodov, I. Kaminer, K. Jones, and I. Kitsios. Rapid motion estimation of a target moving with time-varying velocity. In *AIAA Guidance, Navigation and Control Conference and Exhibit*, August 2007.
- [8] L. Ma, C. Cao, N. Hovakimyan, C. Woolsey, V. Dobrokhodov, and I. Kaminer. Development of a vision-based guidance law for tracking a moving target. In *AIAA Guidance, Navigation and Control Conference and Exhibit*, August 2007.
- [9] Joshua Redding, Timothy W. McLain, Randal W. Beard, and Clark Taylor. Vision-based target localization from a fixed-wing miniature air vehicle. *Journal Of Aerospace Computing, Information, and Communication*, 2(9):348–360, 2005.
- [10] Ruggero Rezza. Path following for air vehicles in coordinated flight. In *International Conference on Advanced Intelligent Mechatronics*, September 1999.
- [11] Rolf Rysdyk. Unmanned aerial vehicle path following for target observation in wind. *Journal of Guidance, Control, and Dynamics*, 29(5):1092–1100, September-October 2006.
- [12] Rolf Rysdyk. Unmanned aerial vehicle path following for target observation in wind. *Journal of Guidance, Control, and Dynamics*, 29(5):1092–1100, September-October 2006.
- [13] Bruno Sinopoli, Mario Micheli, Gianluca Donatot, and T. John Koo\*. Vision based navigation for an unmanned aerial vehicle. *Proceedings of the 2001 IEEE International Conference on Robotics and Automation*, pages 1757–1764, 2001.
- [14] Vahram Stepanyan and Naira Hovakimyan. Visual tracking of a maneuvering target. In *AIAA Guidance, Navigation and Control Conference and Exhibit*, August 2006.
- [15] S. Stolle and R. Rysdyk. Flight path following guidance for unmanned air vehicles with pan-tilt camera for target observation. In *Digital Avionics Systems Conference*, 2003.
- [16] P.G. Thomasson. Guidance of a roll-only camera for ground observation in wind. *Journal of Guidance, Control, and Dynamics*, 21(1):39–44, January-February 1998.
- [17] Ick H. Wang, Vladimir N. Dobrokhodov, Isaac I. Kaminer, and Kevin D. Jones. On vision-based target tracking and range estimation for small UAVs. In *AIAA Guidance, Navigation and Control Conference and Exhibit*, August 2005.